Available online at www.sciencedirect.com
ScienceDirect
Journal of Power Sources 165 (2007) 446–449
JOURNAL OF POWER SOURCES
www.elsevier.com/locate/jpowsour

Short communication

Portable, parallel grid dye-sensitized solar cell module prepared by screen printing

Easwaramoorthi Ramasamy [a,b], Won Jae Lee [a,*], Dong Yoon Lee [a], Jae Sung Song [a]

[a] *Electric and Magnetic Devices Research Group, Korea Electrotechnology Research Institute, P.O. Box 20, Changwon 641-120, Republic of Korea*
[b] *University of Science & Technology, Daejeon 305-333, Republic of Korea*

Received 17 August 2006; accepted 13 November 2006
Available online 9 January 2007

Abstract

Screen-printing technology is used to fabricate large dye-sensitized solar cells (DSSCs). The high series-resistance associated with transparent conductive oxide glass substrates causes poor performance in large DSSCs especially at an exposure of 1 sun. The DSSC design has an embedded silver grid; a fluorine-doped tin oxide (FTO) glass substrate and stripe type titanium dioxide (TiO_2) active layers introduced by screen-printing. The counter electrode is prepared from a screen printable paste based on hexachloro platinic acid. A DSSC module, which consists of five stripe-type working electrodes on a 5 cm × 5 cm, embedded silver grid FTO glass substrate, shows stable performance with an energy conversion efficiency of 5.45% under standard test conditions.

Keywords: Dye-sensitized; Solar cell module; Metal grid; Screen-printing; Efficiency; Embedded silver grid

1. Introduction

Dye-sensitized solar cells (DSSCs) are emerging as low-cost alternatives to conventional, solid-state, silicon solar cells. Following the reasonable energy conversion efficiency that was obtained by using nano-size titanium dioxide (TiO_2) particles [1], interest increased in the possible large-scale application of DSSCs. Even though the performance of DSSCs is inferior to that of conventional solar cells [2], a simple production method at relatively low temperature makes them viable alternative. A schematic diagram of DSSC is shown in Fig. 1. A porous network of a nanosize semiconductor material with a wide band-gaps usually TiO_2, serves as charge transport medium. A monolayer of dye is chemically adsorbed on this material. Photoexcitation of dye causes injection of electrons into the conduction band of TiO_2 from where they diffuse towards a transparent conducting oxide (TCO) substrate. The dye is regenerated through receiving electrons from an iodide/triiodide (I^-/I_3^-) redox couple dissolved in the electrolyte. After passing through a desired load, the electrons enter the cell through a counter electrode to reduce the triiodide ions and thus complete the circuit. Even though 11% efficiency has been achieved with small size cells, commercialization of this technology need to address issues such as dye degradation at elevated temperature, electrolyte leakage, stability, and efficient module design. In recent years, studies have suggested replacement of the liquid electrolyte with a gel or polymer electrolyte [3], a solid-state hole-conducting material [4], or sensitizers that can withstand high temperature [5].

Apart from the conversion of sunlight to electric energy, tandem cells based on DSSC technology can be used in applications such as functional windows [6], water-splitting [7], and photocapacitors [8]. These possibilities have resulted in an increasing amount of research being devoted to the development of large DSSC modules [9,10]. Two types of module design, namely, series interconnect and parallel grid types, appear to be the most promising for the scaling-up of DSSC technology. Series interconnect modules are prepared by connecting individual small cells in series. Since each unit cell is prepared under ideal conditions, it is to be expected that the performance will be the same as

* Corresponding author. Tel.: +82 55 280 1643; fax: +82 55 280 1590.
E-mail address: wjlee@keri.re.kr (W.J. Lee).

0378-7753/$ – see front matter © 2006 Elsevier B.V. All rights reserved.
doi:10.1016/j.jpowsour.2006.11.057

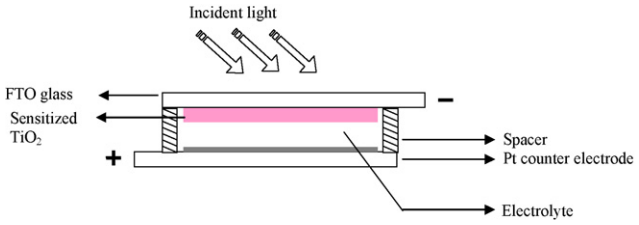

Fig. 1. Schematic diagram of dye-sensitized solar cell.

that of the unit cell. On the other hand, parallel grid modules are prepared on large TCO glass substrates. A device with an active area of a few square centimeters prepared on a fluorine-doped tin oxide (FTO) glass substrate showed an energy conversion efficiency of only 0.3% because of ohmic losses associated with the large substrate [11]. One way to improve the carrier collection and reduce the ohmic losses is to put metal grids on the conducting glass substrate, which is the standard technique employed in silicon solar cell industry [12]. Unfortunately, most of the grid materials are corroded by the redox electrolyte and thus it appears that metal grids need to be protected by means of a protective layer.

In this study, the feasibility of applying a screen-printing method for the preparation of a parallel-type metal grid-embedded DSSC module is examined. For comparison, a plain-type grid-free module is also fabricated on the same size substrate under ideal conditions.

2. Experiment

2.1. Substrate

Fluorine-doped tin oxide glass (Hartford FTO, 80% transmittance in visible region) substrates were used to make both the working and counter electrodes. After successive cleaning in acetone and ethanol, the substrates were dried in a nitrogen atmosphere. Silver grid lines (width × height: 500 μm × 5 μm) were screen printed on the FTO surface using a 200 mesh screen and then dried at 180 °C for 10 min. The distance between the metal grid lines was set to 8 mm. A two-point measurement system showed that the resistance of a 4.5 cm length of silver grid was ∼1 Ω, while that of a bare FTO substrate was ∼30 Ω.

2.2. Electrodes

An active layer that consisted of nanosize TiO_2 (Degussa, P25) in teriphenol and ethyl cellulose was screen printed on a FTO glass substrate. The paste preparation technique is described elsewhere [13]. A screen with a 200 mesh was used to obtain a TiO_2 layer with a thickness of about 10 μm. In order to avoid contamination on fresh film, screen-printing was performed in a clean-room environment. After drying at room temperature for 30 min, the electrodes were sintered at 500 °C for 1 h. After cooling to 80 °C, the electrodes were immersed in a dye solution, namely, cis–bis (isothiocyanato) bis (2,2′-bipyridyl-4,4′-dicarboxylato) ruthenium(II) in absolute ethanol for 24 h. Excess dye was removed by rinsing the electrodes in ethanol. The counter electrode was prepared by printing a thin layer of platinum on a FTO glass substrate by using a paste based on hexachloro platinic acid (Solaronix, Pt-catalyst T/SP) and then sintering at 400 °C for 30 min.

2.3. Device preparation and characterization

A sandwich-type cell was fabricated by assembling a sensitized TiO_2 electrode with a counter electrode. The electrodes were separated by surlyn-based polymer sheet (thickness: 80 μm) and sealed by heating at 100 °C for a few seconds. The liquid electrolyte contained a I^-/I_3^- redox couple in acetonitrile solvent was introduced into the cell via a predrilled hole. The electrolyte injecting holes, made on the counter-electrode side, were sealed with surlyn and a glass cover. The current–voltage characteristic of the DSSCs were measured with a Keithley digital source meter (Model 2400) in both dark and AM 1.5 sunlight illumination. A solar simulator (Oriel) attached with 300 W Xenon lamp was used as the light source. The desired sunlight intensity was achieved by placing a neutral mesh in the optical path. Photographs of a DSSC prepared with a 5 cm × 5 cm FTO glass substrate are given in Fig. 2. A plain cell with a working electrode of dimensions 3.5 cm × 3.5 cm is shown in Fig. 2(a), while a stripe-type cell with active area equivalent to 7 cm^2 is seen in Fig. 2(b).

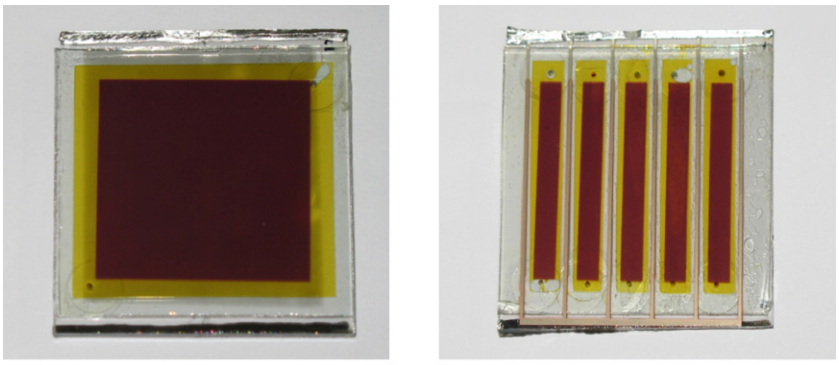

(a) (b)

Fig. 2. Photographs of DSSCs on 5 cm × 5 cm FTO glass substrate with (a) plain-type and (b) stripe-type working electrode.

3. Results and discussion

Scaling-up of DSSC technology without loss of performance at the laboratory scale requires an optimized design of working electrode. If the active area of the device exceeds a few square centimeters, the limited conductivity of the TCO: glass substrate causes an increase in the series resistance and thus affects the fill factor [14]. This effect becomes apparent when the intensity of the incident light approaches the 1-sun level. Given the square type active layer dimensions of the plain-type module, photo-generated carriers have to travel an average distance of 2.5 cm in the FTO glass substrate before reaching the metal contact. This large distance cause an increase in the series resistance and hence influences the fill factor and energy-conversion efficiency of the device. The term fill factor (FF) refers to the ratio of the actual power of the solar cell to the power if both the current and the voltage are at their maximum values. The parameter can be calculated from following relation:

$$\text{fill factor} = \frac{V_m I_m}{V_{oc} I_{sc}} \quad (1)$$

where: V_{oc} is the open-circuit voltage; I_{sc} is the short-circuit current; V_m and I_m are the voltage and the current at the maximum power point, respectively.

The efficiency of sunlight to electric energy conversion of the device is calculated from:

$$\text{efficiency} = \left(\frac{V_{oc} J_{sc}}{P_{in}}\right) \times \text{FF} \quad (2)$$

where J_{sc} is the short-circuit current density and P_{in} is the incident solar radiation, expressed in mW cm^{-2}.

The I–V curve of a plain cell prepared on a 5 cm × 5 cm size FTO glass substrate is shown in Fig. 3(a). Even though device shows reasonable performance with a FF = 60% and η = 2.6 corresponding to 12 mW cm^{-2} illumination, ohmic losses limit the FF to 26% and thus the power-conversion efficiency falls to 1.02% at 1-sun condition. Since power dissipation due to ohmic losses increases as the square of the current flowing through the TCO substrate, this effect is less important at low intensities, yet becomes significant at 1-sun conditions.

One way to overcome ohmic losses is to employ metal grids as in conventional silicon cells and place stripe-type active layers between them. In the case of a DSSC, these metal grid lines should be protected from the corrosive electrolyte by an insulating layer [15]. In this study, serves both functions, surlyn sheet i.e., a spacer and a coating layer for the silver conductive fingers. In this design, the distance between the conductive fingers is set to 8 mm and the stripe-type working electrode (dimensions: 4 mm × 35 mm) is placed between two adjacent conductive fingers. The I–V performance of such a stripe-type device with an active area of 5(3.5 × 0.4) cm^2 is presented in Fig. 3(b). Due to efficient carrier collection, stripe-type devices deliver almost constant performance over the range of illumination conditions. Under low-level illumination, I–V parameters are V_{oc} = 0.66 V, J_{sc} = 0.98 mA cm^{-2}, FF = 68% and efficiency = 3.7%, while similar values are obtained at a 1-sun condition.

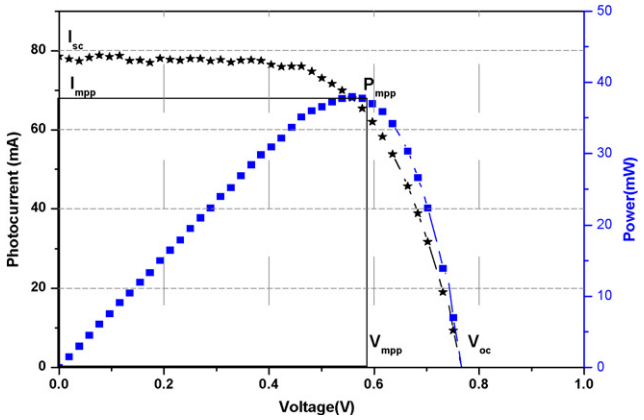

Fig. 4. Power density of stripe-type DSSC module under 1-sun illumination (squares: power density, stars: I–V curve). Power density curve is produced by product of voltage and photocurrent density. P_{mpp} is power density at maximum power point. V_{mpp} and J_{mpp} are voltage and current at maximum power point, respectively.

The power output of the silver grid embedded module is shown in Fig. 4. The maximum peak power is 38 mW. This is three times that of the plain-type module and suggests that the module can be readily used in transparent window applications. It should be noted, however, that the present module is not optimized for high performance, and there is scope for improvement through adjusting the distance between the silver grids and the dimensions of the active layer [16]. Also a non-active area can

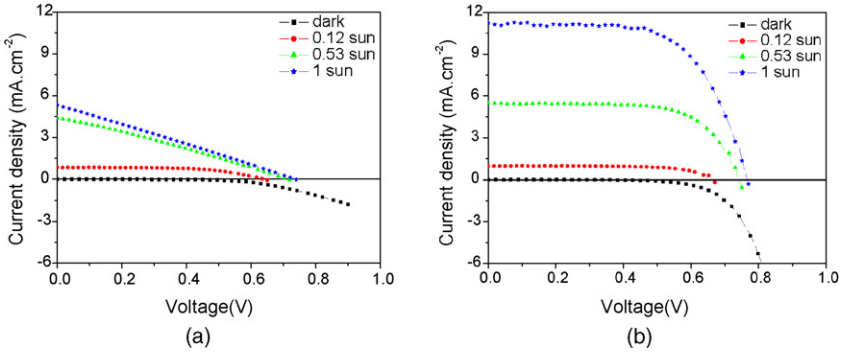

Fig. 3. Current–voltage curves of DSSCs with different types of working electrode on 5 cm × 5 cm FTO glass substrate. (a) Plain cell with active area of 12.25 cm^2, (b) stripe cell with active area of 7 cm^2. Squares represent I–V curve in dark. Circles 12 mW cm^{-2}, triangle-53 mW cm^{-2} and star-100 mW cm^{-2} sunlight intensity.

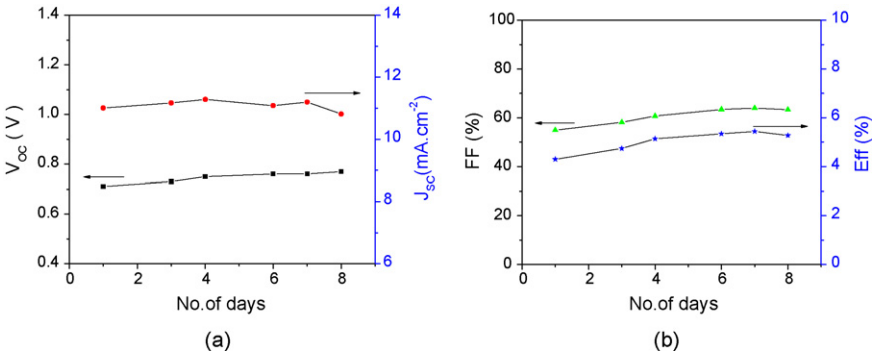

Fig. 5. Variation of I–V parameters of silver grid embedded, stripe-type DSSC module during short-term stability test. (a) Open-circuit voltage V_{oc} and short-circuit current density J_{sc}; (b) fill factor (FF) and energy conversion efficiency (η).

Table 1
I–V parameters of portable DSSC modules under standard test conditions[a]

Parameter	Plain-type	Stripe-type
Active area (cm^2)	12.25	7
Open-circuit voltage (V_{oc})	0.731 V	0.760 V
Short-circuit current density (J_{sc})	5.31 mA cm^{-2}	11.23 mA cm^{-2}
Voltage at maximum power point (V_{mpp})	0.380 V	0.549 V
Current density at maximum power point (J_{mpp})	2.68 mA cm^{-2}	9.91 mA cm^{-2}
Maximum power point (P_{mpp})	1.02 mW cm^{-2}	5.44 mW cm^{-2}
Fill factor (FF)	26.2%	63.8%
Efficiency (η)	1.02%	5.45%

[a] Values are with respect to active area.

be used as a scattering centre for incident photons. Table 1 shows the I–V parameters of the plain- and stripe-type DSSC modules. The typical I–V parameters of a high-performance, commercial silicon solar cell have been reported elsewhere [17].

The performance of the silver grid embedded, stripe-type module during an ageing test are given in Fig. 5. The devices are kept in an ambient atmosphere and the I–V parameters are measured at 24 h intervals. During the first week, the efficiency of the device is slightly enhanced because of an increase in both V_{oc} and FF. It seems that the silver grid lines are perfectly covered and protected against the highly corrosive liquid electrolyte. Short-term stability measurements show that the performance of the silver grid embedded module is in agreement that found in similar studies [18,19]. Also, visual inspection of cells over an extended period confirms that there is no electrolyte leakage from the device.

4. Conclusions

A large dye-sensitized solar cell with moderate efficiency has been fabricated on a silver grid embedded FTO glass substrate by a screen-printing method. Under standard test conditions, an energy conversion efficiency of 5.45% is achieved in a device with an active area equivalent to 7 cm^2. Short-term tests show that the device gives a stable performance. These results illustrate that screen-printing technology can be successfully used in a production line for large DSSCs. The aperture ratio of the present module is 0.27 and is still an order of magnitude lower than that of commercial solar cell modules. It is expected that optimization of the active layer dimensions and the inter-grid distances will enhance the aperture ratio.

References

[1] B. O'Regan, M. Grätzel, Nature 353 (1991) 737–740.
[2] M.A. Green, K. Emery, D.L. King, S. Igari, W. Warta, Prog. Photovoltaics: Res. Appl. 11 (2003) 347–352.
[3] D.W. Kim, Y.B. Jeong, S.H. Kim, D.Y. Lee, J.S. Song, J. Power Sources 149 (2005) 112–116.
[4] U. Bach, D. Lupo, P. Comte, J.E. Moser, F. Weissortel, J. Salbeck, H. Spreitzer, M. Grätzel, Nature 395 (1998) 583–585.
[5] P. Wang, S.M. Zakeerudin, J.E. Moser, M.K. Nazeeruddin, T. Sekiguchi, M. Grätzel, Nature Mater. 2 (2003) 402–407.
[6] C. Bechinger, S. Ferrere, A. Zaban, J. Sprague, B.A. Gregg, Nature 383 (1996) 608–610.
[7] J.H. Park, A.J. Bard, Electrochem. Solid-State Lett. 9 (2006) E5–E8.
[8] T. Miyasaka, T.N. Murakami, Appl. Phys. Lett. 85 (2004) 3932–3934.
[9] G.E. Tulloch, J. Photochem. Photobiol. A: Chem. 164 (2004) 209–219.
[10] R. Sastrawan, J. Beier, U. Belledin, S. Hemming, A. Hinsch, R. Kern, C. Vetter, F.M. Petrat, A. Prodi-Schwab, P. Lechner, W. Hoffmann, Sol. Energy Mater. Sol. Cells 90 (2006) 1680–1691.
[11] K. Okada, H. Matsui, T. Kawashima, T. Ezure, N. Tanabe, J. Photochem. Photobiol. A: Chem. 164 (2004) 193–198.
[12] T. Kaydanova, A. Miedaner, C. Curtis, J. Perkins, J. Alleman, D. Ginley, http://www.nrel.gov/docs/fy03osti/33594.pdf.
[13] W.J. Lee, E. Ramasamy, D.Y. Lee, J.S. Song, J. Photochem. Photobiol. A: Chem. 183 (2006) 133–137.
[14] M.G. Kang, N.G. Park, Y.J. Park, K.S. Ryu, S.H. Chang, Sol. Energy Mater. Sol. Cells 75 (2003) 475–479.
[15] M. Späth, P.M. Sommeling, J.A.M. van Roosmalen, H.J.P. Smit, N.P.G. van der Burg, D.R. Mahieu, N.J. Bakker, J.M. Kroon, Prog. Photovoltaics: Res. Appl. 11 (2003) 207–220.
[16] M. Grätzel, Prog. Photovoltaics: Res. Appl. 8 (2003) 171–185.
[17] IXYS Semiconductor GMBH, Technical Information, http://www.ixys.com/pfslrc01.html.
[18] P. Wang, S.M. Zakeerudin, J.E. Moser, M.K. Nazeeruddin, T. Sekiguchi, M. Grätzel, Nature Mater. 2 (2003) 402–407.
[19] T. Toyoda, T. Sano, J. Nakajima, S. Doi, S. Fukumoto, A. Ito, T. Tohyama, M. Yoshida, T. Kanagawa, T. Motohiro, T. Shiga, K. Higuchi, H. Tanaka, Y. Takeda, T. Fukano, N. Katoh, A. Takeichi, K. Takechi, M. Shiozawa, J. Photochem. Photobiol. A: Chem. 164 (2004) 203–207.